Binding to PI(4,5)P$_2$ is indispensable for secretion of B-cell clonogenic HIV-1 matrix protein p17 variants

Antonella Bugatti[1], Francesca Caccuri[1], Federica Filippini[1], Cosetta Ravelli[2], and Arnaldo Caruso[1,*]

From the [1]Section of Microbiology, [2]Section of Experimental Oncology and Immunology, Department of Molecular and Translational Medicine, University of Brescia Medical School, Brescia, Italy

Edited by Craig Cameron

HIV-1 matrix protein p17 variants (vp17s) derived from non-Hodgkin's lymphoma (NHL) tissues of HIV-1–seropositive (HIV$^+$) patients promote B-cell growth by activating the Akt signaling pathway. It is fundamental to understand the role played by vp17s in producing a microenvironment that fosters lymphoma development and progression. Therefore, we asked whether vp17s could be secreted from infected cells in their biologically active form. In this study, we show that two B-cell growth-promoting vp17s, NHL-a101 and NHL-a102, characterized by amino acid insertions at position 117 to 118 (Ala–Ala) or 125 to 126 (Gly–Asn), respectively, are secreted from HIV-1–infected Jurkat T cells during the active phase of viral replication. Secretion of biologically active vp17s also occurred in HeLa cells nucleofected with a plasmid expressing the entire Gag gene, following proteolytic cleavage of the Gag precursor polyprotein (Pr55^{Gag}) by cellular aspartyl proteases. Binding of Pr55^{Gag} to phosphatidylinositol-(4,5)-bisphosphate was indispensable for allowing the unconventional secretion of both wildtype p17 and vp17s. Indeed, here we demonstrate that inhibition of Pr55^{Gag} binding to phosphatidylinositol-(4,5)-bisphosphate by using neomycin, or its enzymatic depletion achieved by overexpression of 5ptaseIV, significantly impair the secretion of p17s. We also demonstrated that heparan sulfate proteoglycans were involved in tethering p17s at the cell surface. This finding opens up an interesting way for investigating whether tethered p17s on the surface of HIV-1 reservoirs may represent a likely target for immune-mediated killing.

The HIV-1 matrix protein p17 (p17) is a 132 amino acids–long Gag-encoded protein that plays a key role in virus assembly and release (1). Its interaction with many cellular proteins underlines the importance of the viral protein as a major determinant of human-specific adaptation (2). Virion-free p17 is released from HIV-1–infected cells, and it can be detected in blood at nanomolar concentrations (1, 3). Moreover, p17 accumulates and persists in different organs and tissues of patients even under successful combined antiretroviral therapy (cART) (4–6). In particular, a long-term p17 accumulation in lymph nodes of cART-treated patients has

been shown, even after prolonged HIV-1 suppression (4). Taken together, these findings strongly suggest that p17 may be chronically present in the tissue microenvironment of HIV-1–seropositive (HIV$^+$) patients, even during the pharmacological control of viral replication. These findings are consistent with several reports showing that the latently infected resting CD4$^+$ T cells transcribe and translate Gag proteins, even without cell stimulation (7, 8), and that defective HIV-1 proviruses in the CD4$^+$ T cells of HIV$^+$ individuals on cART produce intact Gag proteins in vitro and in vivo (9).

Extracellularly, p17 has been found to deregulate the biological activity of different immune cells, which may be relevant in the context of viral pathogenesis. In particular, p17 is capable of triggering the activation, differentiation, and proliferation of different target immune cells as T cells (10, 11), natural killer cells (12), monocytes (13), and plasmacytoid dendritic cells (3). We also highlighted the capability of p17 to exert chemotactic activity on human primary B cells after binding to the C-X-C motif chemokine receptors 1 and 2 (14, 15). Interestingly, we showed that a p17 variant (vp17) carrying various amino acid substitutions, named S75X, derived from an Ugandan HIV-1 A1 strain, differently from a p17 derived from clade B virus (strain BH10; refp17), activated the Akt signaling pathway in B cells, thereby promoting cell growth and clonogenicity (16). This finding provided the first evidence on the existence of a vp17 with B-cell clonogenic activity on human B cells. More recently, in studies of p17 from human non-Hodgkin's lymphoma (NHL) cases, we characterized two categories of vp17s that promote B-cell growth and activate the Akt pathway: the first characterized by amino acid insertions at position 117 to 118 and the second characterized by amino acid insertions at position 125 to 126 (6). Ultradeep pyrosequencing showed that these two categories of vp17s are more frequently detected in plasma of HIV$^+$ patients with NHL than without NHL (12). Moreover, we showed that vp17s characterized by an Ala–Ala insertion at position 117 to 118 (NHL-a101) and a Gly–Asn insertion at position 125 to 126 (NHL-a102), differently from refp17, were drastically destabilized. Because of misfolding, vp17s were found to expose a common functional epitope with B-cell clonogenic activity located at their N-terminal region (17). Recently, we demonstrated that the B-cell clonogenic activity of both NHL-a101 and NHL-a102 is mediated by activation of

* For correspondence: Arnaldo Caruso, arnaldo.caruso@unibs.it.

the protease-activated receptor 1, which triggers trans-activation of the epidermal growth factor receptor (18). Collectively, our data support the hypothesis that certain vp17s may play a role in lymphoma pathogenesis. It is worth noting that in the cART era, B-cell lymphomas, and NHLs in particular, comprise more than 50% of all AIDS-defining cancers (19) and are still the most frequent cause of death in HIV[+] patients (20), being often characterized by clinical aggressiveness (21, 22).

Despite the lack of signal sequence, similarly to other viral proteins (17, 23–25), p17 is secreted in a biologically active form by an unconventional pathway (26). Its secretion takes place at the plasma membrane of *Gag*-expressing cells, in the absence of active viral proteases. Secretion of p17 was found to be dependent on the interaction of *Gag* precursor polyprotein (Pr55^{Gag}) with phosphatidylinositol-(4,5)-bisphosphate (PI(4,5)P$_2$) and its subsequent cleavage from Pr55^{Gag} operated by cellular aspartyl proteases. We also highlighted that targeting Pr55^{Gag} to the plasma membrane through PI(4,5)P$_2$ interactions is the only feasible mechanism for p17 secretion (26). Several groups have shown the role played by the highly basic region (HBR) located at the p17 N-terminal region in the p17 interaction with PI(4,5)P$_2$ (27–30). Moreover, some Pr55^{Gag} mutants in the HBR showed impaired Pr55^{Gag}–PI(4,5)P$_2$ interaction and relocalization of Pr55^{Gag} from the plasma membrane to intracellular compartments, thus impairing or abolishing p17 secretion (26). Because of their partial unfolding state and remodeling of their N-terminal region to expose the B-cell clonogenic epitope (17), we asked whether interaction of Pr55^{Gag} carrying vp17s with PI(4,5)P$_2$ occurs, leading to Pr55^{Gag} cleavage by cellular or viral proteases and secretion as biologically active proteins. This is critical to hypothesize a role of vp17s in producing a microenvironment that fosters lymphoma development, progression, and metastasis.

Herein, we report that biologically active NHL-a101 and NHL-a102 vp17s are released by cells nucleofected with plasmid-expressing *Gag* or viral mutants. Finally, we show for the first time that secreted refp17 and vp17s are, at least in part, tethered to the cell surface through heparan sulfate proteoglycans (HSPGs).

Results

Quantification of vp17s secretion by T cells

Our first aim was to assess if vp17s secretion occurs during active virus replication. Jurkat cells, which are similar to most HIV-1–infected CD4^{+} T cells (31), were transiently nucleofected with pNL4-3 plasmids expressing refp17, NHL-a101, or NHL-a102 (Jurkat-refp17, Jurkat-NHL-a101, and Jurkat-NHL-a102, respectively). Mock nucleofected cells were used as negative control (Jurkat). Twenty-four hours after nucleofection, 7.5×10^5 cells/well were cultured for additional 24 h in complete medium in anti-p17 mAb MBS-15–coated wells of 96-well plates. Plate-bound p17, secreted by seeded Jurkat-nucleofected cells, was then quantified by ELISA (26). As previously reported, p17 was easily detected in the supernatant of Jurkat-refp17, and the amount of secreted p17 ranged from

3.30 to 3.55 nM (mean ± SD: 3.41 ± 0.10 nM). At the same time, vp17s were also secreted by Jurkat-NHL-a101 (from 1.65 to 2.86 nM, mean ± SD: 2.29 ± 0.57 nM) and Jurkat-NHL-a102 (2.48–3.59 nM, mean ± SD: 3.1 ± 0.39 nM) (Fig. 1). This result attests for the active secretion of refp17 and vp17s from infected cells.

Secreted vp17s are biologically active

We previously demonstrated that differently from refp17, NHL-a101 and NHL-a102 are able to induce B-cell growth and clonogenicity (6). To determine if vp17s are secreted in their biologically active form, we performed a single cell cloning assay on Raji B cells resuspended with supernatants collected from HeLa cells nucleofected with *Gag*-expressing plasmids carrying refp17 (HeLa-refp17), NHL-a101 (HeLa-NHL-a101), or NHL-a102 (HeLa-NHL-a102). As representatively shown in Figure 2A, a visible single colony was spontaneously developing in >60% of seeded wells at day 8 of culture, attesting for active cell proliferation. As expected, in the presence of vp17s released from nucleofected cells, colonies showed a significantly larger size than colonies cultured in medium of mock- or refp17-nucleofected cells.

To demonstrate that the observed B-cell growth and clone expansion was specifically mediated by vp17s, the B-cell cloning assay was performed in the presence or absence of the p17-neutralizing mAb MBS-3, which recognizes the
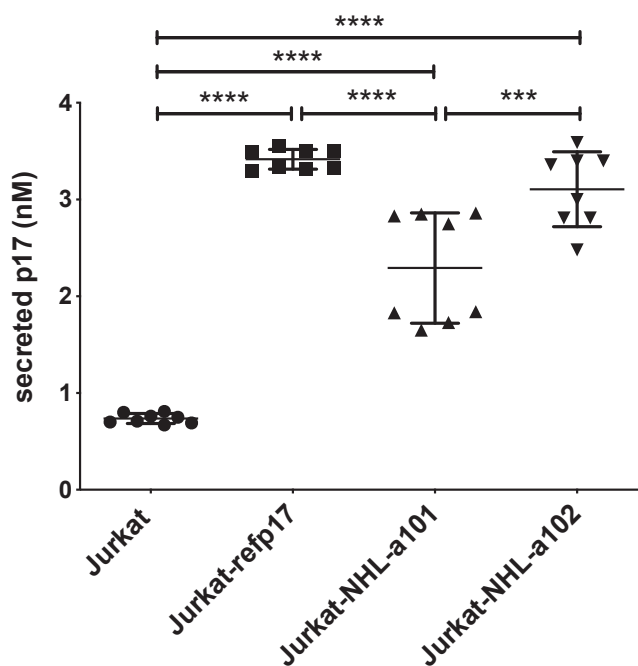

Figure 1. Quantitative p17 secretion assay. Evaluation of p17 release in the cell culture supernatant was performed by cellular ELISA. Jurkat cells were nucleofected with or without the pNL4-3 vector expressing refp17, NHL-a101, or NHL-a102 (Jurkat-refp17, Jurkat-NHL-a101, and Jurkat-NHL-a102, respectively). After 24 h, Jurkat were seeded onto ELISA plates pre-coated with anti-p17 mAb MBS-15 and incubated further for 24 h to allow protein secretion and accumulation. Quantification of released p17s was performed using a standard curve generated with recombinant proteins. Scatter plot was generated using the means of eight independent experiments. One-way ANOVA and the Bonferroni's post-test was used to compare data; ***$p < 0.001$ and ****$p < 0.0001$.
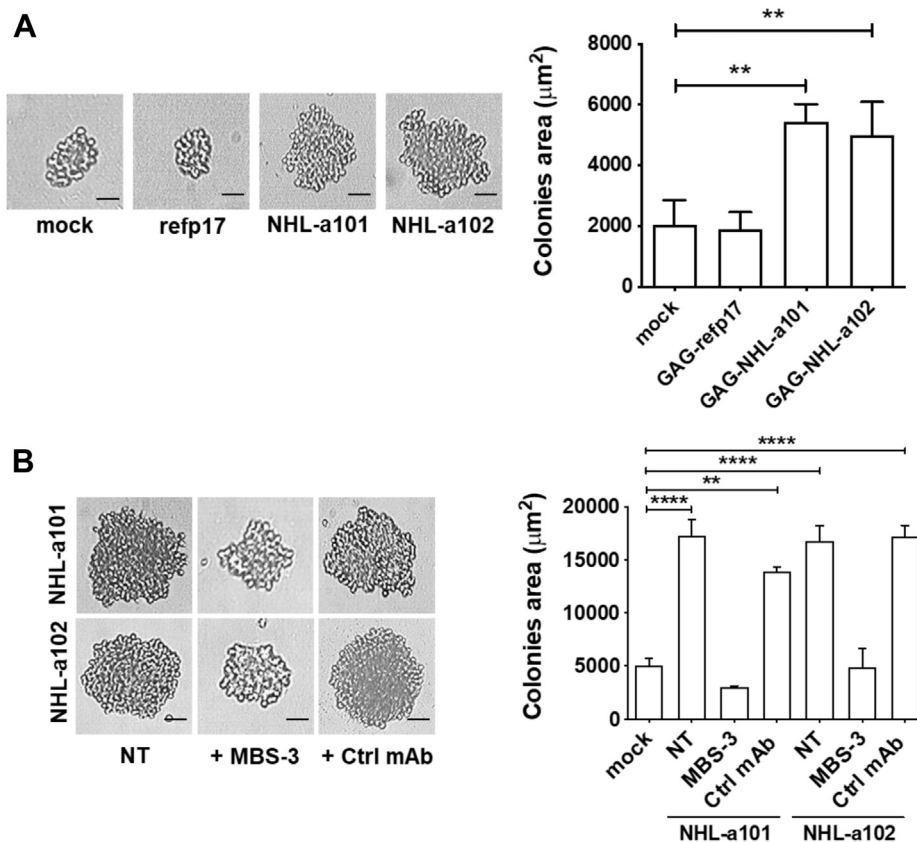
Figure 2. Secreted vp17s induce B-cell growth and transformation. *A*, supernatants collected from HeLa cells nucleofected with *Gag*-expressing plasmids carrying refp17 (HeLa-refp17), NHL-a101 (HeLa-NHL-a101), or NHL-a102 (HeLa-NHL-a102) were used to resuspend Raji B cells (refp17, NHL-a101, and NHL-a102, respectively) and perform colony formation assay. Supernatant collected from mock nucleofected cells (mock) were used as negative control. *B*, for some experimental conditions, HeLa-conditioned supernatants were not treated (NT) or preincubated for 30 min at 37 °C with 1 µg/ml of unrelated Ctrl mAb or p17 neutralizing mAb MBS-3. Bright-field images represent the characteristic morphology of 2D colonies (*left panels*), one colony for each condition is shown (original magnification, 40×). The scale bar represents 25 µM. The colony area was measured (by using Leica Qwin image analysis software [*right panels*]). The graphs were generated using the means of three independent experiments. One-way ANOVA and the Bonferroni's post-test was used to compare data; **$p < 0.01$ and ****$p < 0.0001$. vp17, HIV-1 matrix protein p17 variant.

clonogenic epitope of vp17s (17). An unrelated mAb (Ctrl mAb) was used as negative control in the assay. As representatively shown in Figure 2*B*, the presence of mAb MBS-3 (1 µg/ml) completely inhibited the clonogenic activity of both vp17s, whereas the Ctrl mAb (1 µg/ml) turned out to be ineffective.

We have recently shown that vp17s are biologically active on endothelial cells (ECs) (5, 32). To evaluate whether secreted vp17s were active on ECs, we performed a wound healing assay, by cocultivation of nucleofected HeLa cells and human umbilical vein endothelial cells (HUVECs). A Culture-Insert 2 Well was used to provide two reservoirs for culturing cells that were separated by a 500 µm thick wall. The HUVEC and nucleofected HeLa cells were seeded in the reservoirs and cultured until they attached and formed a monolayer. Removal of the silicone insert from the surface was resulting in two precisely defined cell patches, which were separated by a zone that is exactly the same width as the separation wall. Cell migration of HUVECs was calculated as a percentage of wound observed over a period of 12 h. The number of HUVECs in the wound area increased more quickly (Fig. 3*A*), and the wound area decreased more rapidly in refp17- and vp17s-treated cells as compared with control cells (mock). As

shown in Figure 3*B*, HUVECs cocultivated with mock HeLa cells reached approximately 47% sealing (range from 45 to 49%) after 12 h of culture, whereas, at the same time, HUVECs cocultivated with nucleofected HeLa cells expressing refp17 or its variants reached 80 to 90% sealing. This finding attests for the capability of viral proteins to promote EC migratory activity. Taken together, these data demonstrate that vp17s are secreted from infected cells in their biologically active form.

Secreted p17s accumulate on cellular surface by binding to HSPGs

Recently, we demonstrated that refp17 can be detected inside the cell as a punctate staining at the plasma membrane (26). To evaluate the cellular localization of vp17s, we carried out an indirect immunofluorescence assay and confocal microscopy analysis. HeLa cells were nucleofected with *Gag*-expressing plasmids as described previously (HeLa-refp17, HeLa-NHL-a101, and HeLa-NHL-a102), then fixed, and permeabilized or not before staining with the anti-p17 mAb MBS-3. To avoid mAb MBS-3 internalization, live and not permeabilized cells were maintained on ice during the staining step. Representative confocal images of permeabilized cells
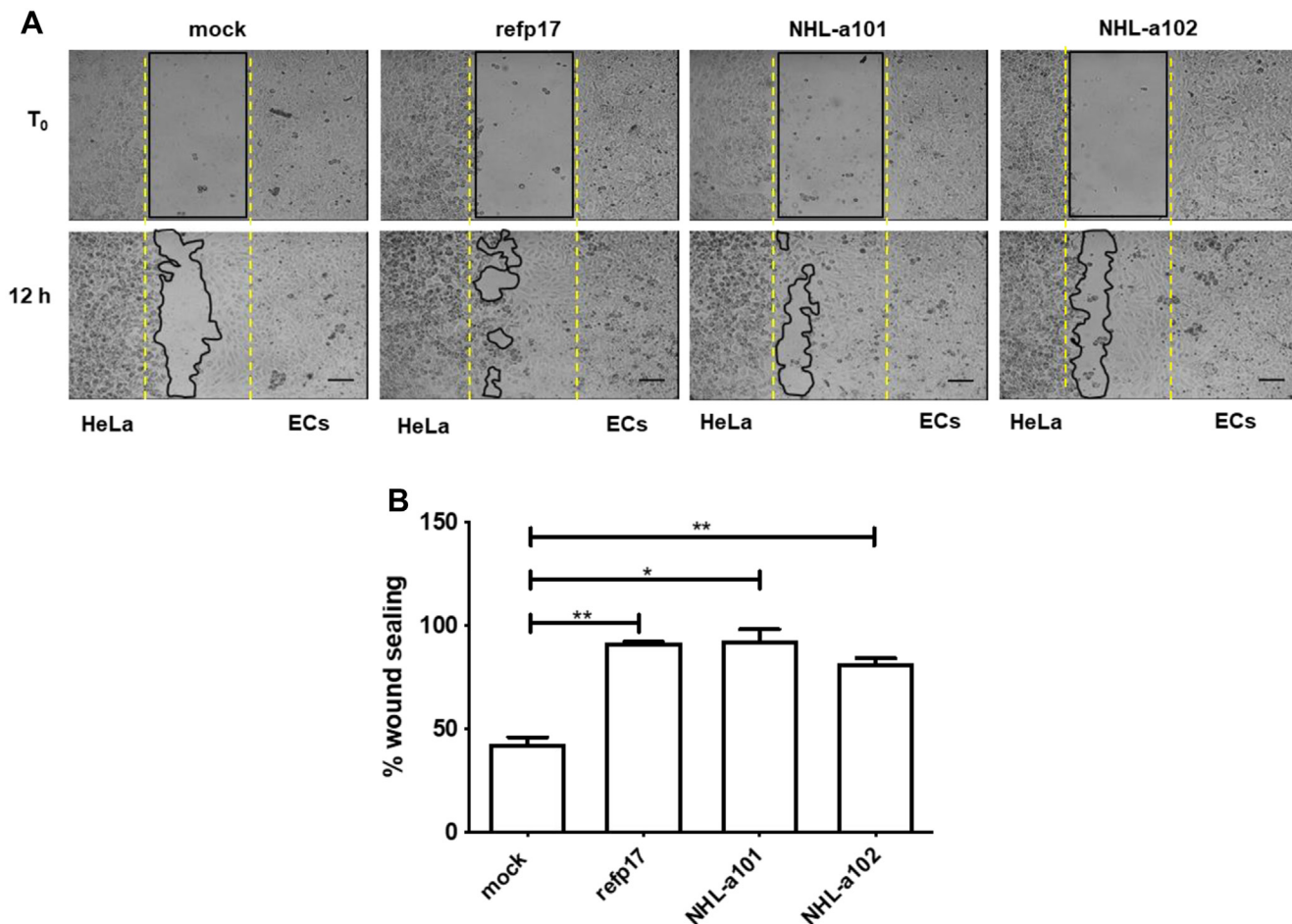
Figure 3. Secreted p17s promote HUVEC migration. *A*, HeLa cells nucleofected with *Gag*-expressing plasmids carrying refp17 (HeLa-refp17), NHL-a101 (HeLa-NHL-a101), or NHL-a102 (HeLa-NHL-a102) were cocultivated with HUVECs in Culture-Insert 2 Well (refp17, NHL-a101, and NHL-a102, respectively). After 24 h of incubation, the insert in the plate was gently removed to create a scratch between HeLa and HUVEC (ECs) cells. Cell migration was recorded by light microscopy over a 12 h time course after wound scratch. Images are representative of three independent experiments with similar results (magnification, 10×). The scale bar represents 100 μm. *B*, graph represents quantitative analysis of wound sealing showing the percentage of the area of the wound at 12 h in relation to the initial total area. Values are the mean ± SD of one representative experiment out of three with similar results. One-way ANOVA and the Bonferroni's post-test was used to compare data; *$p < 0.0$ and **$p < 0.01$. EC, endothelial cell; HUVEC, human umbilical vein endothelial cell.
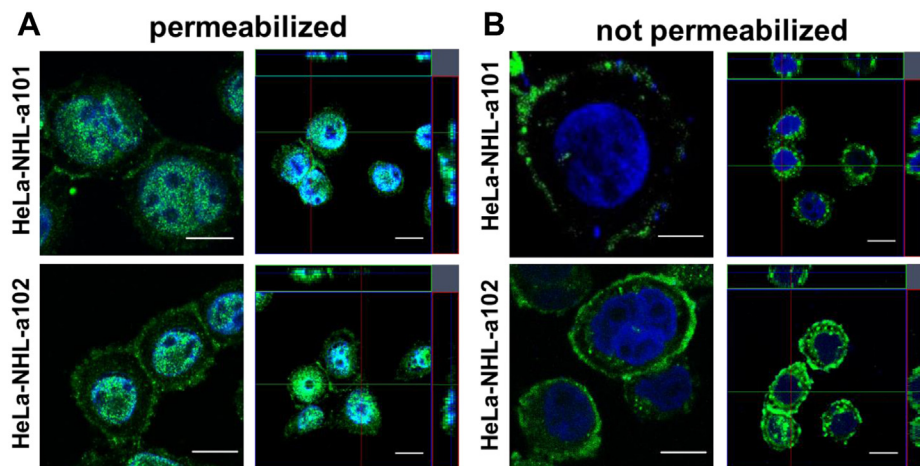

Figure 4. Intracellular localization of vp17s in *Gag*-expressing cells. HeLa cells were nucleofected with *Gag*-expressing plasmids carrying NHL-a101 (HeLa-NHL-a101) or NHL-a102 (HeLa-NHL-a102) and then cultured for 24 h at 37 °C. Cells were (*A*) permeabilized or (*B*) not permeabilized as described in the Experimental procedures section. Cells were then stained with anti-p17 mAb MBS-3 followed by Alexa Fluor 488–conjugated antimouse IgG and 4′,6-diamidino-2-phenylindole. Analysis was performed by confocal fluorescence microscopy. Images display mAb MBS-3 signals in *green* and cell nuclei in *blue*. z-Stack sections and orthogonal z reconstitution are also shown. The scale bar represents 10 μM. vp17, HIV-1 matrix protein p17 variant.

show that vp17s are localized at the plasma membrane as a punctate staining (Fig. 4A), as for refp17. On the contrary, in not permeabilized HeLa cells, both vp17s are confined on cell surface only (Fig. 4B). Previously, we have shown that refp17 is able to bind the HSPGs because of the presence of two distinct heparin-binding domains (33). To scrutinize the binding of vp17s to HSPGs, we performed a surface plasmon resonance (SPR) assay with heparin bound on the sensor chip. As shown in Figure 5A, both vp17s were found to bind heparin in a dose-dependent manner. The sensorgram overlay shown in Figure 5A allowed the calculation of association (K_{on}) and dissociation (K_{off}) rates and of K_d (as K_{off}/K_{on} ratio) (Table 1). Based on this evidence, we hypothesize that HSPGs could be involved in vp17s binding on the cellular surface. Then, live and not permeabilized nucleofected HeLa cells were maintained for 24 h in the presence or absence of soluble heparin (10 µg/ml) or washed with 2 M NaCl (salt wash) before staining for indirect immunofluorescence assay. As shown in Figure 5B, not permeabilized cells treated with soluble heparin or salt washed, completely lost the expression of refp17 and vp17s on the cell surface, as compared with not treated cells. This finding suggests for the key role played by HSPGs in tethering refp17 and vp17s on cellular surface following their secretion.

Secretion of vp17s takes place directly at the plasma membrane level following binding to PI(4,5)P₂

We previously showed that *Gag* can be processed in the absence of HIV-1 protease being p17 digested from Pr55^{Gag} by cellular intramembrane aspartyl proteases following its binding to PI(4,5)P₂, and that this process represents an essential step in promoting refp17 secretion (25). To evaluate if secretion of vp17s follows the same mechanism observed with refp17 in the absence of HIV-1 protease, we treated nucleofected HeLa-NHL-a101 and HeLa-NHL-a102 with soluble neomycin sulfate, a polycationic aminoglycoside antibiotic that binds to PI(4,5)P₂ impairing the binding of PI(4,5)P₂ ligands by steric hindrance (34), and pepstatin A, an inhibitor of cellular aspartyl proteases (35).

As shown in Figure 6A, permeabilized HeLa-NHL-a101 and HeLa-NHL-a102 showed vp17s expression as a punctate staining at the plasma membrane. On the contrary, neomycin-treated cells showed a diffuse p17 expression in the cytoplasm. At the same time, pepstatin A treatment showed a dispersed vp17s expression within the cell cytoplasm and more pronounced at the plasma membrane (Fig. 6A). This result suggests that neomycin and pepstatin A favor intracellular vp17s accumulation by interfering with its enzymatic cleavage from Pr55^{Gag}, as already observed in refp17-expressing cells (26). To further prove that vp17s secretion mechanism depends on the binding of viral proteins to PI(4,5)P₂ at the cellular plasma membrane, we examined p17 secretion in cells depleted for PI(4,5)P₂ by overexpression of 5ptaseIV (36). As shown in Figure 6A, HeLa-NHL-a101 and HeLa-NHL-a102 over-expressing 5ptaseIV displayed a diffuse distribution of vp17s in the cytoplasm. In contrast, HeLa-NHL-a101 and HeLa-NHL-a102 overexpressing the mutant form of 5ptseIV (5ptaseIV-Δ1) showed a punctate staining at the plasma membrane. These results are in agreement with previous data obtained with HeLa-refp17 (26).
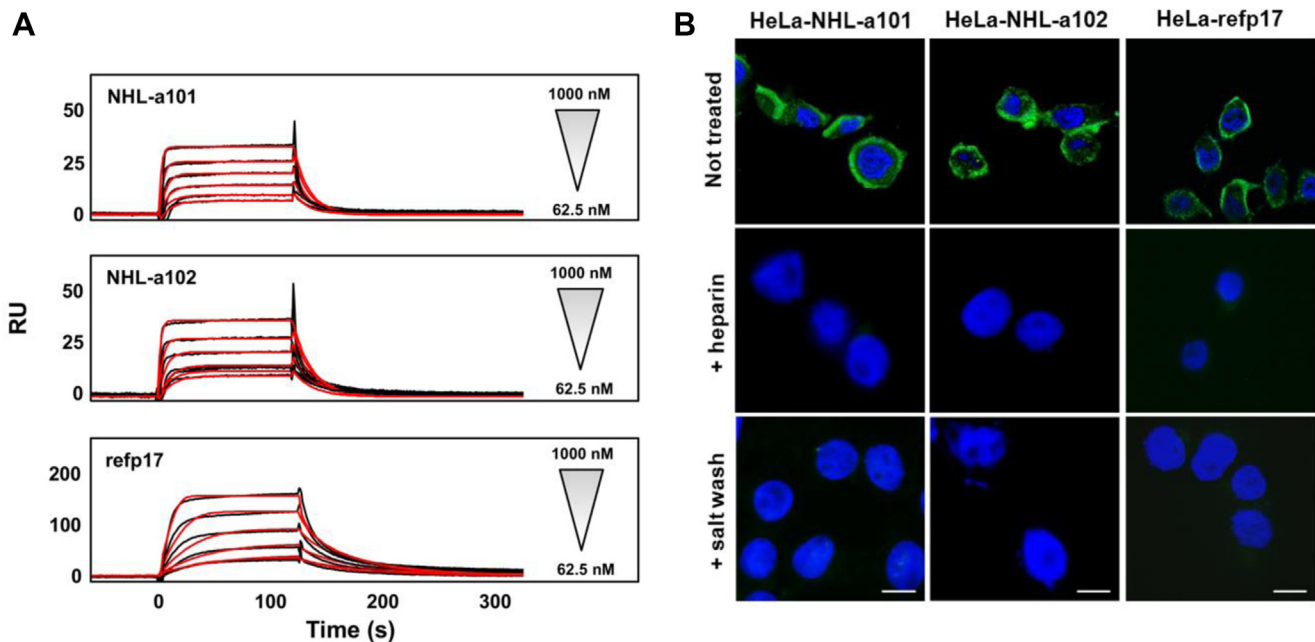

Figure 5. P17s associate with cellular HSPGs. *A*, binding of p17s to heparin analyzed by SPR. Refp17 and its variants were injected on heparin sensor chip surface. All the proteins were tested at increasing concentrations (from 62.5 to 1000 nM). Affinity values of interaction were determined by BIAevaluation software. *B*, HeLa cells were nucleofected with *Gag*-expressing plasmids carrying refp17 (HeLa-refp17), NHL-a101 (HeLa-NHL-a101), or NHL-a102 (HeLa-NHL-a102) and then either incubated for 24 h in the presence of soluble heparin (10 µg/ml) or washed with PBS supplemented with 2 M NaCl (salt wash). Not permeabilized cells were then stained with anti-p17 mAb MBS-3 followed by Alexa Fluor 488–conjugated antimouse IgG and 4′,6-diamidino-2-phenylindole. Analysis was performed by fluorescence microscopy. Images display mAb MBS-3 signals in *green* and cell nuclei in *blue*. The scale bar represents 5 µm. HSPG, heparan sulfate proteoglycan; SPR, surface plasmon resonance.

ASBMB

J. Biol. Chem. (2021) 297(2) 100934 **5**

Table 1
The association rate (K_{on}) and dissociation rate (K_{off}) are reported and the dissociation constant (K_d) was derived from the K_{off}/K_{on} ratio

Protein	Association rate (K_{on})	Dissociation rate (K_{off})	Dissociation constant (K_d)
	1/Ms	1/s	M
NHL-a101	8.84E + 5	0.077	8.71E − 8
NHL-a102	8.41E + 5	0.059	7.01E − 8
refp17	2.62E + 5	0.148	5.64E − 8

In order to understand if refp17 and vp17s are secreted following their binding to PI(4,5)P$_2$ during HIV-1 replication, we analyzed the effect of neomycin and pepstatin A on secretion of viral proteins following nucleofection with plasmids expressing the wildtype HIV-1 or HIV-1 mutants carrying NHL-a101 or NHL-a102 vp17s. As shown in Figure 6B, neomycin and pepstatin A were found to significantly inhibit the secretion of both NHL-a101 and NHL-a102 vp17s as well as of refp17, compared with untreated cells, thus confirming that the inhibition of Pr55^{Gag} binding to PI(4,5)P$_2$ or its enzymatic cleavage prevents the release of vp17s. We then examined the impact of PI(4,5)P$_2$ depletion on vp17s secretion by cellular ELISA. As shown in Figure 6C, secretion of refp17 and vp17s was strongly impaired in overexpressing 5ptaseIV. At the same time, Jurkat-refp17, Jurkat-NHL-a101, and Jurkat-NHL-a102 overexpressing 5ptaseIV-Δ1 released p17 at concentrations not significantly different from those detected in the supernatant of control cells, thus confirming the key role played by PI(4,5)P$_2$ in vp17s secretion.
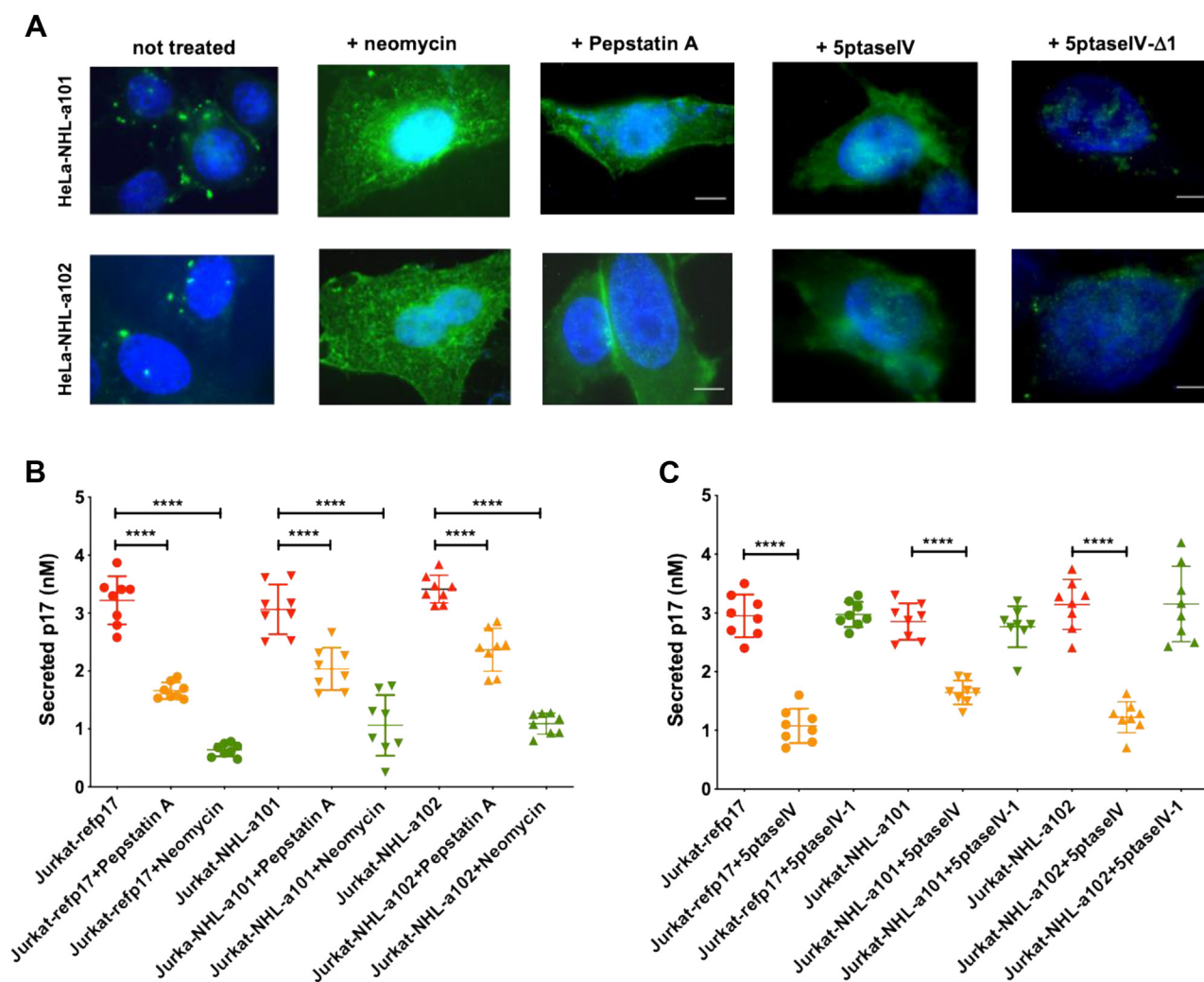

Figure 6. Secretion of vp17s requires PI(4,5)P$_2$ binding at the plasma membrane level. *A*, HeLa cells were nucleofected with *Gag*-expressing plasmids carrying NHL-a101 (HeLa-NHL-a101) or NHL-a102 (HeLa-NHL-a102) and treated with pepstatin A (10 µM) or neomycin (500 µM). In some experiments, HeLa-NHL-a101 and HeLa-NHL-a102 were conucleofected with 5ptaseIV or 5ptaseIV-Δ1 mutant expression plasmids. Twenty-four hours later, permeabilized cells were stained with anti-p17 mAb MBS-3 followed by Alexa Fluor 488–conjugated antimouse IgG and 4′,6-diamidino-2-phenylindole. Analysis was performed by fluorescence microscopy. Images display mAb MBS-3 signals in *green* and cell nuclei in *blue*. The scale bar represents 5 µm. *B*, Jurkat cells were nucleofected with the pNL4-3 vector expressing refp17, NHL-a101, or NHL-a102 (Jurkat-refp17, Jurkat-NHL-a101, and Jurkat-NHL-a102, respectively) and treated or not with pepstatin A (10 µM) or neomycin (500 µM). *C*, Jurkat-refp17, Jurkat-NHL-a101, or Jurkat-NHL-a102 was conucleofected with 5ptaseIV or 5ptaseIV-Δ1 mutant expression plasmids. The evaluation of released vp17s was performed by cellular ELISA. Scatter plot was generated using the means of eight experiments. One-way ANOVA and the Bonferroni's post-test was used to compare data; ****$p < 0.0001$. PI(4,5)P$_2$, phosphatidylinositol-(4,5)-bisphosphate; vp17, HIV-1 matrix protein p17 variant.

Discussion

In light of the emerging role of the microenvironment in promoting and sustaining the growth and survival of tumor cells ([37], [38]), the possibility that HIV-1–encoded proteins derived from infected cells and endowed with peculiar biologic properties contribute to lymphomagenesis was entertained. A previous study has shown that a vp17 increases cell proliferation of Epstein–Barr virus–infected primary human B cells ([39]). Moreover, a more recent analysis showed a potential role of vp17s in promoting lymphoma in HIV[+] patients, thus providing a rational explanation for the paradox of persistent risk for lymphoma among patients despite the immune-restorative effects of cART. Indeed, biologically active vp17s capable of augmenting clonogenic proliferation of lymphoma cell lines were detected in lymphoma tissue of patients with NHL and mirrored in their plasma counterparts ([6]).

Refp17 is released in a biologically active form by *Gag*-expressing cells, and secretion of the viral protein takes place at the plasma membrane, following refp17 interaction with $PI(4,5)P_2$. The release of refp17 occurs following its cleavage from $Pr55^{Gag}$ by cellular aspartyl proteases ([26]). Here, we show for the first time that two different vp17s, characterized by amino acid insertion at position 117 to 118 or 125 to 126, are secreted following the same unconventional mechanism previously described for refp17. Moreover, we show that vp17s are secreted in a biologically active form by both infected and *Gag*-nucleofected cells, as attested by their ability to trigger B-cell proliferation and transformation and promote EC migration. This finding attests that secretion of vp17s can occur both in the presence or the absence of active viral proteases. In the latter case, secretion of vp17s was found to be promoted by cellular aspartyl proteases–operated cleavage and be depending on the vp17s binding to $PI(4,5)P_2$. In particular, our data show that $Pr55^{Gag}$ binding to $PI(4,5)P_2$ on plasma membrane is an essential step in promoting vp17s cleavage and secretion and that reduction of cellular $PI(4,5)P_2$ levels by 5ptaseIV overexpression strongly impaired vp17s secretion. Previous findings showed the critical role of specific amino acids included in the HBR in refp17–$PI(4,5)P_2$ interaction and/or in stabilizing such interaction and consequently allowing refp17 secretion. In particular, mutation of Lys at position 30 and 32 was found to strongly affect $Pr55^{Gag}$–$PI(4,5)P_2$ interaction and refp17 secretion, whereas Trp mutation at position 36 completely abolished p17 secretion. This latter finding can be, at least in part, explained by the knowledge that the side chain of W36 interacts with the glycerol moiety and with the C4-acyl chain of $PI(4,5)P_2$ ([27]). It is worth noting that W36 is a highly conserved amino acid and possibly evolutionarily relevant, given that it is maintained in its ancestor simian immunodeficiency virus matrix protein, whose extracellular biological activities have been recently found to resemble, for many aspects, those of the HIV-1 vp17s ([15]). The evidence that these critical amino acid residues are well preserved on the primary sequence of both NHL-a101 and NHL-a102 explain how such high conservation, which occurs for all p17 amino acid residues strictly involved in $PI(4,5)P_2$ interaction, may be necessary for sites that interact with cellular constituents that do not undergo

evolutionary changes on the timescale of HIV-1 replication. Clonogenic vp17s are destabilized as compared with refp17 ([6], [16]). This suggests that protein destabilization, induced by mutations (deletions and insertions included) not restricted to the C terminus of p17, may ensue a conformational change sufficient to endow the NH_2-terminal region of the viral protein with B-cell growth-promoting activity, presumably through better protease-activated receptor 1 recruitment and activation. At the same time, conformational changes in the N-terminal region do not alter the $PI(4,5)P_2$ interacting epitope, which is indispensable for HIV-1 envelope incorporation and particle assembly at the plasma membrane ([29], [40]).

It has been demonstrated that even during HIV-1 latency, cells can produce *Gag* polyproteins without supporting virus assembly and spreading of infection being sufficient for the presence of unspliced RNA to allow the nuclear export and translation of *Gag* ([9]). This knowledge is supported by the evidence that *Gag* can be processed in the absence of HIV-1 protease ([26]) and give rise to p17 proteins capable of being released, in a biologically active form, in the extracellular microenvironment. These findings, together with the recent evidence showing the persistence of defective proviruses in HIV-infected individuals during cART capable of producing HIV viral proteins ([8]), contribute to the evidence that vp17s can be released also during HIV-1 latency leading to lymphatic B-cell stimulation, growth, and transformation. Popovic *et al.* ([4]) previously demonstrated persistence of p17 but not viral RNA in lymph nodes of patients on cART who were virally suppressed, suggesting the presence of soluble p17 in these tissues. If so, the impact of vp17s on B-cell growth and transformation is likely to persist. Recent data have highlighted the capability of vp17s to also promote both angiogenesis and lymphangiogenesis ([41], [42]), which are essential in supporting proliferation and survival of lymphoma, as well as tumor cell dissemination ([43]). Altogether, these evidences corroborate the hypothesis that vp17s actively secreted may be stored within a variety of organs and tissues where they may likely function as promoter of B-cell growth and transformation. Derived from our data are fundamental insights into the molecular basis on the key role that vp17s may play in lymphomagenesis, calls for inhibiting the biological activity of vp17s. This may be achieved in the microenvironment, by inoculating neutralizing antibodies ([17]), or by using specific therapeutic vaccines ([44]) aimed to generate a strong and efficient neutralizing antibody response. But it may be possibly realized also at the intracellular level, by avoiding $Pr55^{Gag}$–$PI(4,5)P_2$ interaction through anti-p17 antibody gene transduction ([45]) or small-molecule inhibitors able to engage the $PI(4,5)P_2$ binding pocket of the viral protein ([46]).

In this study we show, for the first time, that both refp17 and vp17s are secreted in the extracellular environment but are also tethered to the cell surface through HSPGs. Amount of viral proteins associated with HSPGs, in addition to the free protein in the plasma, could represent a way to interact with specific receptors expressed on other—not necessarily infected—cells, and possibly cause bystander activation and dysfunction. In this view, it is likely that cell–cell contact can be

implicated in promoting the highly efficient direct passage of the viral protein from one cell to another, acting as a virological synapse. Manipulation of the synapse may prevent an effective immune response to the virus, similarly to previous observation of evasion strategies by which Nef prevents recognition of infected cells by cytotoxic T lymphocytes and with other effects of the viral protein on cytokine secretion by macrophages and dendritic cells (47). On the other hand, the finding of p17 tethering on the surface of HIV-1 reservoirs may offer new opportunities to promote the development of therapeutic strategies aimed to HIV-1 eradication. Up to date, one of the most prominent approaches to achieve HIV-1 cure with the aim of reducing the viral reservoir is "shock and kill," which uses latency reversing agents to induce viral gene expression and productive infection in latently infected cells, exposing those cells to immune clearance or to the viral cytopathic effect (48). Expression of p17 on the surface of infected cells in the absence of active virus replication may ultimately represent a target for immune-mediated clearing ("kill"), thus allowing elimination of viral reservoirs even in the absence of HIV-1 latency reversal. This hypothesis needs to be validated in suitable *in vitro* and *in vivo* models of HIV-1 latency.

Experimental procedures

Expression vectors

pNL4-3 vector, containing a full infectious provirus, HIV-1$_{NL4-3}$, was a kind gift of Dr Anna Cereseto (University of Trento, Italy). Tat-independent AG49CMVIL15-RTEm26CTE vector was kindly provided by Dr Barbara Felber (National Cancer Institute, Frederick). The *Gag*-expressing plasmid AG49CMV*Gag*-RTEm26CTE was generated as previously described (26). The plasmids carrying vp17s, namely NHL-a101 and NHL-a102, were generated by substituting the refp17 within the *Gag* gene, with vp17s synthetic genes (Integrated DNA Technologies). Cells nucleofected without plasmid were used as negative control (mock). The 5ptaseIV expression plasmid, pcDNA4TO/Myc5ptaseIV, was a gift from P. Majerus (Washington University School of Medicine, St Louis, MO). The 5ptaseIV mutant lacking the phosphatase signature domain (Δ1) was a gift from A. Ono (University of Michigan Medical School, Ann Arbor, MI).

Recombinant proteins and mAbs to p17

Monomeric HIV-1 matrix protein p17 and its variants were produced and purified as previously described (16). The absence of endotoxin contamination (<0.25 endotoxin units/ml) in protein preparations was assessed by Limulus amoebocyte assay (Associates of Cape Cod). mAbs to p17 (neutralizing mAbs: MBS-3 and MBS-34; not neutralizing mAbs: MBS-15 MBS-55) were produced in our laboratory (5, 49).

Cells

HeLa, Jurkat, and Raji cell lines (American Type Culture Collection) were maintained in RPMI1640 (Merck) supplemented with 10% fetal bovine serum (FBS) (Merck), sodium

pyruvate, and L-glutamine (2 mM). HUVECs have been previously developed and characterized (5). Cells were cultured in endothelial cell growth medium (EGM) supplemented with 10% FBS. All the experiments were carried out with cells at passages 2 to 6. Cells were maintained at 37 °C in a humidified atmosphere of 5% CO_2.

vp17s secretion assay

Jurkat cells were nucleofected using the Amaxa Nucleofector II device (Lonza) and the Ingenio Electroporation Universal kit (Mirus). Twenty-four hours after nucleofection, cells were washed with RPMI1640, resuspended in complete medium, and then transferred to an ELISA MaxiSorp Nunc plate (7.5 × 10^5 cells/well, in triplicate) previously coated overnight at 4 °C with the anti-p17 mAb MBS-15 at 10 µg/ml in PBS. After 24 h of incubation, cells were removed and biotinylated anti-p17 mAb (MBS-55 or MBS-34 [1 µg/ml] for NHL-a101 and NHL-a102, respectively) was added to the wells for 1 h at 37 °C. Detection of immunocomplexes was performed using a peroxidase-labeled streptavidin (BD Biosciences) and the 3,3,5,5-tetramethylbenzidine (Merck) as chromogenic substrate. Standard curves for p17 and its variants were generated by serial dilution of the recombinant proteins (from 0.125 to 18 nM), and the amount of secreted p17s was calculated by linear interpolation. In some experiments, nucleofected cells were treated with neomycin (500 µM) [as PI(4,5)P2 inhibitor] (Life Technologies) and pepstatin A (10 µM) (as inhibitor of aspartyl proteases) (Merck). When reported, Jurkat cells were conucleofected with the 5ptaseIV expression plasmid pcDNA4TO/Myc5ptaseIV66 or with the mutant expression plasmid pcDNA4TO/Myc Δ15ptaseIV (36, 50).

B-cell colony formation assay

HeLa cells were nucleofected with *Gag* plasmid expressing refp17, NHL-a101, or NHL-a102. Twenty-four hours later, cell supernatants were collected and centrifuged to remove cell debris. The clarified medium was used to perform the colony formation assay (17). Raji cells resuspended in conditioned supernatants were seeded by manual pipetting into a 96-well plate at a dilution of 0.5 cells/well. When reported, conditioned supernatants were preincubated for 30 min at 37 °C with 1 µg/ml of unrelated Ctrl mAb or p17 neutralizing mAb MBS-3. After 8 days of incubation, the culture plates were analyzed for single colony formation.

Wound healing assay

The Culture-Insert 2 Well (Ibidi GmbH) was used to perform the assay. In the first well, HUVEC cells were plated (1 × 10^5 cells/well) in EGM containing 10% FBS, and confluent cell monolayers were starved for 24 h by replacing medium with endothelial basal medium containing 0.5% FBS. In the second well, HeLa cells (1 × 10^5 cells/well) were plated after nucleofection with *Gag* plasmid expressing refp17, NHL-a101, or NHL-a102. Twenty-four hours later, the Culture-Insert 2 Well were gently removed with sterile tweezers creating a physical gap within the two cell monolayers. Cell layers were

washed with PBS to remove cell debris and not attached cells. The µDish was filled with cell medium (EGM supplemented with 10% FBS) applying the recommended volume of 2 ml. HUVEC migration in response to refp17 or variant proteins secreted by nucleofected HeLa cells was evaluated at different time points using an inverted microscope (DM-IRB microscope system; Leica). HUVECs migrating into the wounded area, or protruding from the border of the wound, were photographed using a charge-coupled device camera (Hitachi, Inc) connected to a computer. The areas of the wound were calculated by using the ImageJ software (National Institutes of Health).

Immunofluorescence analysis

HeLa cells were nucleofected with AG49CMV*Gag*-RTEm26CTE plasmid expressing refp17, NHL-a101, or NHL-a102 (HeLa-ref, HeLa-NHL-a101, and HeLa-NHL-a102, respectively), cultured for 24 h in complete medium, and then stained for immunofluorescence as follows: fixed with 3% paraformaldehyde/2% sucrose in PBS for 30 min, permeabilized with 0.5% Triton, and saturated with 1% bovine serum albumin (BSA) in PBS. Then, the cells were incubated for 1 h with the anti-p17 mAb MBS-3 followed by Alexa Fluor 488–conjugated antimouse IgG (Molecular Probes) at room temperature. When indicated, not fixed cells were saturated with 1% BSA in PBS, incubated for 1 h with the anti-p17 mAb MBS-3 followed by Alexa Fluor 488–conjugated antimouse IgG on ice and then fixed as aforementioned. Nuclei were counterstained with 4′,6-diamidino,2-phenylindole (DAPI; Sigma). When reported, nucleofected HeLa cells were also treated with neomycin (500 µM) [as PI(4,5)P2 inhibitor] (Life Technologies) or with the specific cellular aspartyl protease inhibitor pepstatin A (10 µM) (Merck). In some experiments, HeLa cells were conucleofected with the 5ptaseIV expression plasmid pcDNA4TO/Myc5ptaseIV66 or with the mutant expression plasmid pcDNA4TO/Myc Δ15ptaseIV. In selected experiments, cells were treated with 10 µg/ml of the conventional unmodified heparin (13.6 kDa) (Laboratori Derivati Organici S.p.A.) or salt washed with 2 M NaCl (Sigma). Fluorescence was recorded with a Nikon DXM 1200 digital camera system (Nikon) coupled to the Eclipse E1000 fluorescence microscope (Nikon) and the ACT-1 control software (Nikon).

Confocal analysis

HeLa cells were nucleofected with AG49CMVGag-RTEm26CTE plasmid expressing NHL-a101 or NHL-a102 (HeLa-NHL-a101 and HeLa-NHL-a102, respectively), cultured for 24 h in complete medium, and then stained for confocal microscopy analysis as follows: fixed with 3% paraformaldehyde/2% sucrose in PBS for 30 min, permeabilized with 0.5% Triton, and saturated with 1% BSA in PBS. Then, the cells were incubated for 1 h with the anti-p17 mAb MBS-3 followed by Alexa Fluor 488–conjugated antimouse IgG (Molecular Probes) at room temperature. When indicated, not fixed cells were saturated with 1% BSA in PBS, incubated for

1 h with the anti-p17 mAb MBS-3 followed by Alexa Fluor 488–conjugated antimouse IgG on ice and then fixed as aforementioned. Nuclei were counterstained with DAPI (Sigma). Cells were analyzed using a Zeiss LSM510 Meta confocal microscope equipped with a Plan-Apochromat 63×/1.4 numerical aperture oil objective. The excitation sources were an argon ion and 405-nm diode lasers for Alexa Fluor 488 and DAPI, respectively. Alexa Fluor 488 was acquired using a LP 505 filter, whereas DAPI was acquired using a LP 420 combined with an NFT 490 beam splitter. Single images and orthogonal projection from z-stack sections were obtained through Zen Black 2 software (Zeiss).

SPR experiments

SPR measurements were conducted on a Biacore X100 (GE Healthcare) at 25 °C. SPR was used to characterize the binding of HIV-1 p17s to heparin immobilized on a sensor chip. Biotinylated heparin was immobilized onto a SA sensor chip containing preimmobilized streptavidin, allowing the immobilization of 115 resonance units, equal to 8.5 fmol/mm^2 of heparin. A sensor chip precoated with streptavidin alone was used to evaluate nonspecific binding and for blank subtraction ([51]). Increasing concentrations of p17 or its variants in 10 mM Hepes, pH 7.4 containing 150 mM NaCl, 3 mM EDTA, and 0.005% surfactant P20 (HBS-EP) were injected over the heparin or streptavidin surfaces for 4 min and then washed until dissociation. After each run, the sensor chip was regenerated by injection of 2 M NaCl in HBS-EP. Kinetic parameters were calculated from the sensorgram overlays by using the nonlinear fitting single-site model software package BIAevaluation (version 3.2 [GE Healthcare]). Only sensorgrams whose fitting gave χ^2 values close to 10 were used ([52]).

Statistical analysis

Data obtained from multiple independent experiments are expressed as the mean ± SD. Data were analyzed for statistical significance using the one-way ANOVA. Bonferroni's post-test was used to compare data. Differences were considered significant at $p < 0.05$. Statistical tests were performed using GraphPad Prism 8 software (GraphPad Software, Inc).

Data availability

All data have been included within the article.

ASBMB

J. Biol. Chem. (2021) 297(2) 100934 **9**

Abbreviations—The abbreviations used are: BSA, bovine serum albumin; cART, combined antiretroviral therapy; DAPI, 4′,6-diamidino,2-phenylindole; EC, endothelial cell; EGM, endothelial cell growth medium; FBS, fetal bovine serum; HBR, highly basic region; HSPG, heparan sulfate proteoglycan; HUVEC, human umbilical vein endothelial cell; NHL, non-Hodgkin's lymphoma; p17, HIV-1 matrix protein p17; (PI(4,5)P$_2$), phosphatidylinositol-(4,5)-bisphosphate; Pr55^{Gag}, precursor Gag polyprotein; SPR, surface plasmon resonance; vp17, HIV-1 matrix protein p17 variant.

References

1. Fiorentini, S., Marini, E., Caracciolo, S., and Caruso, A. (2006) Functions of the HIV-1 matrix proteins p17. *New Microbiol.* **29**, 1–10
2. Caccuri, F., D'Ursi, P., Uggeri, M., Bugatti, A., Mazzuca, P., Zani, A., Filippini, F., Salmona, M., Ribatti, D., Slevin, M., Orro, A., Lu, W., Liò, P., Gallo, R. C., and Caruso, A. (2021) Evolution toward beta common chain receptor usage links the matrix proteins of HIV-1 and its ancestors to human erythropoietin. *Proc. Natl. Acad. Sci. U. S. A.* **118**, e2021366118
3. Fiorentini, S., Riboldi, E., Facchetti, F., Avolio, M., Fabbri, M., Tosti, G., Becker, P. D., Guzman, C. A., Sozzani, S., Caruso, A., and Fiorentini, S. (2008) HIV-1 matrix protein p17 induces human plasmacytoid dendritic cells to acquire a migratory immature cell phenotype. *Proc. Natl. Acad. Sci. U. S. A.* **105**, 3867–3872
4. Popovic, M., Tenner-Racz, K., Pelser, C., Stellbrink, H.-J., Van Lunzen, J., Lewis, G., Kalyanaraman, V. S., Gallo, R. C., Racz, P., and Popovic, M. (2005) Persistence of HIV-1 structural proteins and glycoproteins in lymph nodes of patients under highly active antiretroviral therap. *Proc. Natl. Acad. Sci. U. S. A.* **102**, 14807–14812
5. Caccuri, F., Giagulli, C., Bugatti, A., Benetti, A., Alessandri, G., Ribatti, D., Marsico, S., Apostoli, P., Slevin, M. A., Rusnati, M., Guzman, C. A., Fiorentini, S., and Caruso, A. (2012) HIV-1 matrix protein p17 promotes angiogenesis via chemokine receptors CXCR1 and CXCR2. *Proc. Natl. Acad. Sci. U. S. A.* **109**, 14580–14585
6. Dolcetti, R., Giagulli, C., He, W., Selleri, M., Caccuri, F., Eyzaguirre, L. M., Mazzuca, P., Corbellini, S., Campilongo, F., Marsico, S., Giombini, E., Muraro, E., Rozera, G., De Paoli, P., Carbone, A., *et al.* (2015) Role of HIV-1 matrix protein p17 variants in lymphoma pathogenesis. *Proc. Natl. Acad. Sci. U. S. A.* **112**, 14331–14336
7. Vandergeeten, C., Quivy, V., Moutschen, M., Van Lint, C., Piette, J., and Legrand-Poels, S. (2007) HIV-1 protease inhibitors do not interfere with provirus transcription and host cell apoptosis induced by combined treatment TNF-alpha + TSA. *Biochem. Pharmacol.* **73**, 1738–1748
8. Pace, M. J., Graf, E. H., Agosto, L. M., Mexas, A. M., Male, F., Brady, T., Bushman, F. D., and O'Doherty, U. (2012) Directly infected resting CD4+T cells can produce HIV Gag without spreading infection in a model of HIV latency. *PLoS Pathog.* **8**, e1002818
9. Imamichi, H., Smith, M., Adelsberger, J. W., Izumi, T., Scrimieri, F., Sherman, B. T., Rehm, C. A., Imamichi, T., Pau, A., Catalfamo, M., Fauci, A. S., and Lane, H. C. (2020) Defective HIV-1 proviruses produce viral proteins. *Proc. Natl. Acad. Sci. U. S. A.* **117**, 3704–3710
10. De Francesco, M. A., Caruso, A., Fallacara, F., Canaris, A. D., Dima, F., Poiesi, C., Licenziati, S., Corulli, M., Martinelli, F., Fiorentini, S., and Turano, A. (1998) HIV p17 enhances lymphocyte proliferation and HIV-1 replication after binding to a human serum factor. *AIDS* **12**, 245–252
11. De Francesco, M. A., Baronio, M., Fiorentini, S., Signorini, C., Bonfanti, C., Poiesi, C., Popovic, M., Grassi, M., Garrafa, E., Bozzo, L., Lewis, G. K., Licenziati, S., Gallo, R. C., and Caruso, A. (2002) HIV-1 matrix protein p17 increases the production of proinflammatory cytokines and counteracts IL-4 activity by binding to a cellular receptor. *Proc. Natl. Acad. Sci. U. S. A.* **99**, 9972–9977
12. Vitale, M., Caruso, A., De Francesco, M. A., Rodella, L., Bozzo, L., Garrafa, E., Grassi, M., Gobbi, G., Cacchioli, A., and Fiorentini, S. (2003) HIV-1 matrix protein p17 enhances the proliferative activity of natural killer cells and increases their ability to secrete proinflammatory cytokines. *Br. J. Haematol.* **120**, 337–343
13. Marini, E., Tiberio, L., Caracciolo, S., Tosti, G., Guzman, C. A., Schiaffonati, L., Fiorentini, S., and Caruso, A. (2008) HIV-1 matrix protein p17 binds to monocytes and selectively stimulates MCP-1 secretion: Role of transcriptional factor AP-1. *Cell. Microbiol.* **10**, 655–666
14. Giagulli, C., Magieram, A. K., Bugatti, A., Caccuri, F., Marsico, S., Rusnati, M., Vermi, W., Fiorentini, S., and Caruso, A. (2012) HIV-1 matrix protein p17 binds to the IL-8 receptor CXCR1 and shows IL-8–like chemokine activity on monocytes through Rho/ROCK activation. *Blood* **119**, 2274–2283
15. Caccuri, F., Giagulli, C., Reichelt, J., Martorelli, D., Marsico, S., Bugatti, A., Barone, I., Rusnati, M., Guzman, C. A., Dolcetti, R., and Caruso, A. (2014) Simian immunodeficiency virus and human immunodeficiency virus type 1 matrix proteins specify different capabilities to modulate B cell growth. *J. Virol.* **88**, 5706–5717
16. Giagulli, C., Marsico, S., Magiera, A. K., Bruno, R., Caccuri, F., Barone, I., Fiorentini, S., Andò, S., and Caruso, A. (2011) Opposite effects of HIV-1 p17 variants on PTEN activation and cell growth in B cells. *PLoS One* **6**, e17831
17. He, W., Mazzuca, P., Yuan, W., Varney, K., Bugatti, A., Cagnotto, A., Giagulli, C., Rusnati, M., Marsico, S., Diomede, L., Salmona, M., Caruso, A., Lu, W., and Caccuri, F. (2018) Identification of amino acid residues critical for the B cell growth-promoting activity of HIV-1 matrix protein p17 variants. *Biochim. Biophys. Acta Gen. Subj.* **1863**, 13–24
18. Giagulli, C., Caccuri, F., Zorzan, S., Bugatti, A., Zani, A., Filippini, F., Manocha, E., D'Ursi, P., Orro, A., Dolcetti, R., and Caruso, A. (2020) B-cell clonogenic activity of HIV-1 p17 variants is driven by PAR1-mediated EGF transactivation. *Cancer Gene Ther.* **28**, 649–666
19. Shiels, M. S., Pfeiffer, R. M., Gail, M. H., Hall, H. I., Li, J., Chaturvedi, A. K., Bhatia, K., Uldrick, T. S., Yarchoan, R., Goedert, J. J., and Engels, E. A. (2011) Cancer burden in the HIV-infected population in the United States. *J. Natl. Cancer Inst.* **103**, 753–762
20. Vandenhende, M. A., Roussillon, C., Henard, S., Morlat, P., Oksenhendler, E., Aumaitre, H., Georget, A., May, T., Rosenthal, E., Salmon, D., Cacoub, P., Costagliola, D., Chène, G., Bonnet, F., and ANRS EN20 Mortalité 2010 Study Group (2015) Cancer-related causes of death among HIV-infected patients in France in 2010: Evolution since 2000. *PLoS One* **10**, e0129550
21. Coté, T. R., Biggar, R. J., Rosenberg, P. S., Devesa, S. S., Percy, C., Yellin, F. J., Lemp, G., Hardy, C., Geodert, J. J., and Blattner, W. A. (1997) Non-Hodgkin's lymphoma among people with AIDS: Incidence, presentation and public health burden. AIDS/Cancer Study Group. *Int. J. Cancer* **73**, 645–650
22. Knowles, D. M. (2003) Etiology and pathogenesis of AIDS-related non-Hodgkin's lymphoma. *Hematol. Oncol. Clin. North. Am.* **17**, 785–820
23. Johnson, K. A., Taghon, G. J., Scott, J. L., and Stahelin, R. V. (2016) The Ebola virus matrix protein, VP40, requires phosphatidylinositol 4,5-bisphosphate (PI(4,5)P2) for extensive oligomerization at the plasma membrane and viral egress. *Sci. Rep.* **6**, 19125
24. Mori, T., Mineta, Y., Aoyama, Y., and Sera, T. (2008) Efficient secretion of the herpes simplex virus tegument protein VP22 from living mammalian cells. *Arch. Virol.* **153**, 1191–1195
25. Alefantis, T., Mostoller, K., Jain, P., Harhaj, E., Grant, C., and Wigdahl, B. (2005) Secretion of the human T cell leukemia virus type I transactivator protein tax. *J. Biol. Chem.* **280**, 17353–17362
26. Caccuri, F., Iaria, M. L., Campilongo, F., Varney, K., Rossi, A., Mitola, S., Schiarea, S., Bugatti, A., Mazzuca, P., Giagulli, C., Fiorentini, S., Lu, W., Salmona, M., and Caruso, A. (2016) Cellular aspartyl proteases promote the unconventional secretion of biologically active HIV-1 matrix protein p17. *Sci. Rep.* **6**, 38027
27. Saad, J. S., Miller, J., Tai, J., Kim, A., Ghanam, R. H., and Summers, M. F. (2006) Structural basis for targeting HIV-1 Gag proteins to the plasma membrane for virus assembly. *Proc. Natl. Acad. Sci. U. S. A.* **103**, 11364–11369
28. Chukkapalli, V., Hogue, I. B., Boyko, V., Hu, W. S., and Ono, A. (2008) Interaction between the human immunodeficiency virus type 1 Gag matrix domain and phosphatidylinositol-(4,5)-bisphosphate is essential for efficient Gag membrane binding. *J. Virol.* **82**, 2405–2417

29. Chukkapalli, V., Oh, S. J., and Ono, A. (2010) Opposing mechanisms involving RNA and lipids regulate HIV-1 Gag membrane binding through the highly basic region of the matrix domain. *Proc. Natl. Acad. Sci. U. S. A.* **107**, 1600–1605

30. Shkriabai, N., Datta, S. A., Zhao, Z., Hess, S., Rein, A., and Kvaratskhelia, M. (2006) Interactions of HIV-1 Gag with assembly cofactors. *Biochemistry* **45**, 4077–4083

31. Stebbing, J., Gazzard, B., and Douek, D. C. (2004) Where does HIV live? *N. Engl. J. Med.* **350**, 1872–1880

32. Mazzuca, P., Marsico, S., Schulze, K., Mitola, S., Pils, M. C., Giagulli, C., Guzman, C. A., Caruso, A., and Caccuri, F. (2017) Role of autophagy in HIV-1 matrix protein p17-driven lymphangiogenesis. *J. Virol.* **91**, e00801–e00817

33. Bugatti, A., Giagulli, C., Urbinati, C., Caccuri, F., Chiodelli, P., Oreste, P., Fiorentini, S., Orro, A., Milanesi, L., D'Ursi, P., Caruso, A., and Rusnati, M. (2012) Molecular interaction studies of hiv-1 matrix protein p17 and heparin identification of the heparin-binding motif of p17 as a target for the development of multitarget antagonists. *J. Biol. Chem.* **288**, 1150–1161

34. Gabev, E., Kasianowicz, J., Abbott, T., and McLaughlin, S. (1989) Binding of neomycin to phosphatidylinositol 4,5-bisphosphate (PIP2). *Biochim. Biophys. Acta* **979**, 105–112

35. Marciniszyn, K., and Chang, W. J. (1997) Pepstatin inhibition mechanism. *Adv. Exp. Med. Biol.* **95**, 199–210

36. Kisseleva, M. V., Cao, L., and Majerus, P. W. (2002) Phosphoinositide-specific inositol polyphosphate 5-phosphatase IV inhibits Akt/protein kinase B phosphorylation and leads to apoptotic cell death. *J. Biol. Chem.* **277**, 6266–6272

37. Taylor, J. G., Liapis, K., and Gribben, J. G. (2015) The role of the tumor microenvironment in HIV associated lymphomas. *Biomark. Med.* **9**, 473–482

38. Isaguliants, M., Bayurova, E., Avdoshina, D., Kondrashova, A., Chiodi, F., and Palefsky, J. M. (2021) Oncogenic effects of HIV-1 proteins, mechanisms behind. *Cancers (Basel).* **13**, 305

39. Martorelli, D., Muraro, E., Mastorci, K., Dal Col, J., Faè, D. A., Furlan, C., Giagulli, C., Caccuri, F., Rusnati, M., Fiorentini, S., Carbone, A., Caruso, A., and Dolcetti, R. (2015) A natural HIV p17 protein variant upregulates the LMP-1 EBV oncoprotein and promotes the growth of EBV-infected B-lymphocytes:implications for EBV-driven lymphomagenesis in the HIV setting. *Int. J. Cancer* **137**, 1374–1385

40. Ono, A., Orenstein, J. M., and Freed, E. O. (2000) Role of the gag matrix domain in targeting human immunodeficiency virus type 1 assembly. *J. Virol.* **74**, 2855–2866

41. Caccuri, F., Rueckert, C., Giagulli, C., Schulze, K., Basta, D., Zicari, S., Marsico, S., Cervi, E., Fiorentini, S., Slevin, M., Guzman, C. A., and Caruso, A. (2014) HIV-1 matrix protein p17 promotes lymphangiogenesis and activates the endothelin-1/endothelin B receptor axis. *Arterioscler. Thromb. Vasc. Biol.* **34**, 846–856

42. Basta, D., Latinovic, O., Lafferty, M. K., Sun, L., Bryant, J., Lu, W., Caccuri, F., Caruso, A., Gallo, R., and Garzino-Demo, A. (2015) Angiogenic, lymphangiogenic and adipogenic effects of HIV-1 matrix protein p17. *Pathog. Dis.* **73**, ftv062

43. Pepper, M. S., Tille, J. C., Nisato, R., and Skobe, M. (2003) Lymphangiogenesis and tumor metastasis. *Cell. Tissue Res.* **314**, 167–177

44. Iaria, M. L., Fiorentini, S., Focà, E., Zicari, S., Giagulli, C., Caccuri, F., Francisci, D., Di Perri, G., Castelli, F., Baldelli, F., and Caruso, A. (2014) Synthetic HIV-1 matrix protein p17-based AT20-KLH therapeutic immunization in HIV-1-infected patients receiving antiretroviral treatment: A phase I safety and immunogenicity study. *Vaccine* **32**, 1072–1078

45. Tewari, D., Notkins, A. L., and Zhou, P. (2003) Inhibition of HIV-1 replication in primary human T cells transduced with an intracellular anti-HIV-1 p17 antibody gene. *J. Gene Med.* **5**, 182–189

46. Zenter, I., Sierra, L., Fraser, A. K., Maciunas, L., Mankowski, M. K., Vinnik, A., Fedichev, P., Ptak, R. G., Martin-Garcia, J., and Cockln, S. (2013) Identification of a small-molecule inhibitor of HIV-1 assembly that targets the phosphatidylinositol (4,5)-bisphosphate binding site of the HIV-1 matrix protein. *ChemMedChem* **8**, 426–432

47. Fackler, O. T., Alcover, A., and Schwartz, O. (2007) Modulation of the immunological synapse: A key to HIV-1 pathogenesis? *Nat. Rev. Immunol.* **7**, 310–317

48. Deeks, S. G. (2012) HIV: Shock and kill. *Nature* **487**, 439–440

49. Fiorentini, S., Marsico, S., Becker, P. D., Iaria, M. L., Bruno, R., Guzmán, C. A., and Caruso, A. (2008) Synthetic peptide AT20 coupled to KLH elicits antibodies against a conserved conformational epitope from a major functional area of the HIV-1 matrix protein p17. *Vaccine* **26**, 4758–4765

50. Zhou, W., and Resh, M. D. (1996) Differential membrane binding of the human immunodeficiency virus type 1 matrix protein. *J. Virol.* **70**, 8540–8548

51. Rusnati, M., Urbinati, C., Caputo, A., Possati, L., Lortat-Jacob, H., Giacca, M., Ribatti, D., and Presta, M. (2001) Pentosan polysulfate as an inhibitor of extracellular HIV-1 Tat. *J. Biol. Chem.* **276**, 22420–22425

52. Rusnati, M., and Urbinati, C. (2009) Polysulfated/sulfonated compounds for the development of drugs at the crossroad of viral infection and oncogenesis. *Curr. Pharm. Des.* **15**, 2946–2957

ASBMB

J. Biol. Chem. (2021) 297(2) 100934 **11**